Real-time control of electron cyclotron wave polarization in the LHD

T. Ii Tsujimura[a,*], Y. Mizuno[a], T. Tokuzawa[a], Y. Ito[a], S. Kubo[a], T. Shimozuma[a], Y. Yoshimura[a], H. Igami[a], H. Takahashi[a,b], A. Ejiri[c], the LHD Experiment Group[a]

[a] *National Institute for Fusion Science, National Institutes of Natural Sciences, Toki 509-5292, Japan*
[b] *SOKENDAI (The Graduate University for Advanced Studies), Toki 509-5292, Japan*
[c] *Graduate School of Frontier Sciences, The University of Tokyo, Kashiwa 277-8561, Japan*

Abstract

Peripheral plasma with finite electron density gradients and finite magnetic shear is known to affect polarization of electron cyclotron (EC) waves. Calculation of the ratio between the ordinary (O) mode and the extraordinary (X) mode, integrated in the ray-tracing code developed for EC heated plasmas in the Large Helical Device (LHD), enables the search for the optimum EC wave polarization in order to excite the pure O/X mode at the EC resonance layer. The real-time control system of the incident polarization was developed for maximum single-pass absorption of EC waves, based on the dependence of optimum EC wave polarization on peripheral density profiles. The polarization control system is equipped with a fast field programmable gate array, which processes in real time the calculation of the peripheral electron density profile and the optimum EC wave polarization for motion control of the polarization rotator and the elliptical polarizer on the transmission line. The real-time control in LHD experiments functioned properly in maintaining the absorbed power of the EC wave higher than that without the control, demonstrating that the purer heating mode was successfully excited.

Keywords: ECRH, polarization, real-time control, mode content analysis, FPGA, LHD

1. Introduction

In electron cyclotron resonance heating (ECRH) experiments on the Large Helical Device (LHD), attempts have been made to adjust the deposition location or the incident wave polarization of ECRH, which have contributed to obtaining high electron temperature plasmas and fulfilling demands from a physical point of view [1, 2]. The post-processing ray-tracing calculation with the "LHDGauss" code after every discharge using ECRH provides not only the deposition location but also the ratio between the ordinary (O) mode and the extraordinary (X) mode of each electron cyclotron (EC) wave [3]. The distinctive feature of this code is that the O/X-mode ratio is calculated by solving the one-dimensional (1D) full-wave equation with a given polarization along propagation through the plasma peripheral region from each launching antenna to the EC resonance layer in the LHD. The feature clarified that the O/X-mode ratio is affected by the existence of finite electron density gradients and strong magnetic shear at the plasma peripheral region outside the last closed flux surface (LCFS) [4, 5]. Thus, exciting the pure O mode or the pure X mode at the EC resonance layer requires optimization of the incident wave polarization depending on the peripheral plasma. The impact of a plasma peripheral region on pure excitation of the O/X mode as well as on refraction of rays is a common characteristic in magnetically confined plasmas with comparable scale lengths for the electron density gradients and change of the magnetic shear, such as in the stochastic region of LHD plasmas or in tokamak plasmas at the pedestal region or the SOL (scrape-off-layer). This effect is important in order for effective absorption of EC wave power and to prevent damage to inner vessel components from the undesired stray wave radiation.

As physical quantities such as the electron density evolve in time during a single discharge, the optimum incident polarization or the optimum launching direction for effective absorption of EC waves can change in time accordingly, although in most experiments those settings are fixed during a discharge. Trials of feedforward polarization control and real-time control of the deposition location of EC waves have been recently made during ECRH discharges at ASDEX Upgrade for their specific objectives [6, 7]. The characteristic of the deposition location control is that fast beam-tracing calculations are performed in real time. In the LHD, experiments were carried out for feedforward polarization control [5], feedback steering mirror control [8], and feedback polarization control [9]. The electron temperature measured with the electron cyclotron emission (ECE) diagnostic was used as a reference signal for their feedback control. It is obvious, however, that only the changes of the deposition location or the polarization of EC waves do not always change the ECE temperature. For example, fueling or magnetohydrodynamic instabilities can change the ECE temperature. Even if launching parameters of the EC waves are reaching their optima, the ECE temperature can decrease due to other causes. The situation can give rise to an increased stray radiation level due to the

*Corresponding author
Email address: tsujimura.tohru@nifs.ac.jp (T. Ii Tsujimura)

launching parameters set away from their optima. Although power-modulation ECRH and resultant modulated ECE signals help to evaluate the accurate deposition location, fast estimation of the deposition location is necessary for real-time control purposes and losing ECRH power during modulation is an inefficient use of a gyrotron for steady-state operations.

An idea arises for achieving effective absorption of EC waves: an incident EC wave polarization can be optimized by real-time control using a reference data set regarding peripheral plasmas with different electron density profiles with the help of the recently upgraded ray-tracing code LHDGauss. This method is based on the power absorption model of EC waves, thereby contributing to future upgrades of the numerical model by comparison with experimental results and to more secure use of the ECRH system. This paper describes real-time control of the incident EC wave polarization using this method. Section 2 describes the real-time control system of the incident EC wave polarization. In section 3, results on proof-of-principle experiments of the real-time control are presented and discussed. Section 4 summarizes this paper.

2. Real-time control system of incident EC wave polarization

It is reported in incident polarization scan experiments using the 77 GHz EC wave launched from the 5.5-U (upper) port of the LHD that the polarization under the highest absorbed power obtained experimentally is in good agreement with that optimized in the mode content analysis with LHDGauss [3, 4, 5]. The fundamental O mode at 77 GHz is used for plasma heating under the standard magnetic field configuration of the magnetic axis of $R_{\mathrm{ax}} = 3.6$ m and the magnetic field strength of $B_{\mathrm{t}} = 2.75$ T. In order to excite the pure O mode at the EC resonance layer, the optimum incident EC wave polarization is calculated by solving the 1D full-wave equation along the inverse propagating direction, i.e., the direction from the right-handed wave (R) cutoff point to the launching antenna center, under the initial condition of the O-mode polarization. Taking into account the peripheral region outside the LCFS for the calculation results in good agreement with the experimental results.

Based on these results, the dependence of the optimum incident polarization on the electron density profile in the peripheral region outside the LCFS, as shown in Fig. 1, is adopted as a real-time control model of the incident polarization. In Fig. 1, the electron density profile outside the LCFS is modeled as an exponentially decaying function with $n_{\mathrm{e,LCFS}}$ as the electron density at the LCFS and $\lambda_{n,\mathrm{path}}$ as the scale length for the density gradients along the EC beam path. The polarization state is expressed with the polarization rotation angle α and the ellipticity β. Here, α is defined as the rotation angle to the axis, whose base vector is directed to $-\boldsymbol{k}\times(\boldsymbol{k}\times\boldsymbol{\varphi})$, which is almost the toroidal direction for launch from the 5.5-U port at the LHD. $\boldsymbol{k}$ and $\boldsymbol{\varphi}$ denote the wavenumber and the toroidal direction, respectively. $(\alpha_{\mathrm{opt}},\beta_{\mathrm{opt}})$ is the polarization state at the launching antenna center optimized to excite the pure O mode. The incident EC wave polarization can be

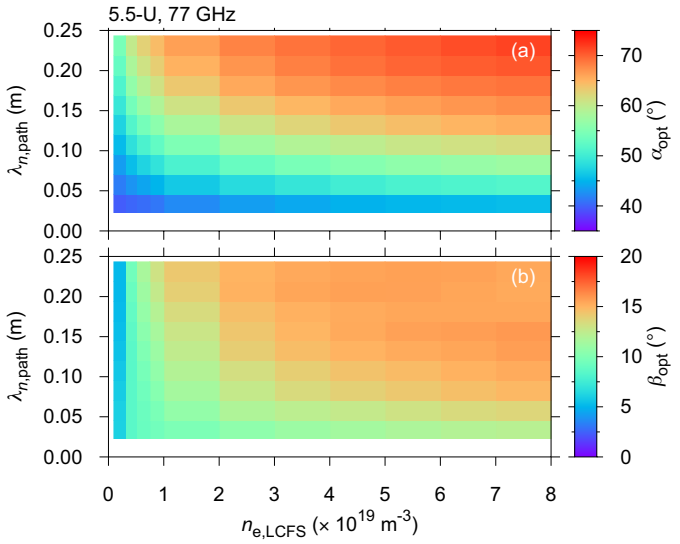

Figure 1: Dependence of optimum incident EC wave polarization on peripheral density profile: (a) the optimum polarization rotation angle α_{opt} and (b) the optimum polarization ellipticity β_{opt} for different electron density $n_{\mathrm{e,LCFS}}$ at the LCFS and the scale length for the density gradients $\lambda_{n,\mathrm{path}}$ along the EC beam path.

adjusted during a discharge according to the dependence on those two parameters regarding the peripheral electron density profile in order for maximum single-pass absorption of the EC wave. This kind of dependence is generally applicable to other magnetic configurations, launcher locations, or gyrotron frequencies in magnetically confined fusion devices.

The multi-channel far-infrared (FIR) laser interferometer [10] is applicable to real-time diagnostics during long-pulse operations on the LHD, so that it is adopted to obtain the peripheral density profile in real time. Figure 2 illustrates the developed real-time control system of the incident EC wave polarization. The real-time polarization control under real-time acquisition of the density profile is performed with real-time FPGA (field programmable gate array) processing, which is realized using a fast reliable hardware CompactRIO (cRIO) cRIO-9035 and its input/output modules made by National Instruments and its software through LabVIEW FPGA programming. The data set on the dependence of the optimum polarization on the peripheral density profile, as shown in Fig. 1, as well as the data set on the relationship between the optimum polarization and the rotation angles of the polarization rotator and the elliptical polarizer on the transmission line are saved into the FPGA memories in advance and referred to in real time. It is noted that there is not less than one combination of the rotation angles of the two polarizers in order to realize a polarization state [11]. Thus, the combination is selected so that the polarizers can rotate seamlessly during the real-time control. The maximum rotation speed of each polarizer is 200°/s. Each polarizer mirror is mounted on a rotating stage (Nikka Densok PF100-CHF-G1), whose worm gear ratio is 180:1. The stage is connected to a low-inertia servo motor and its amplifier (Panasonic MSME012G1N and MADHT1505), whose maximum rotation

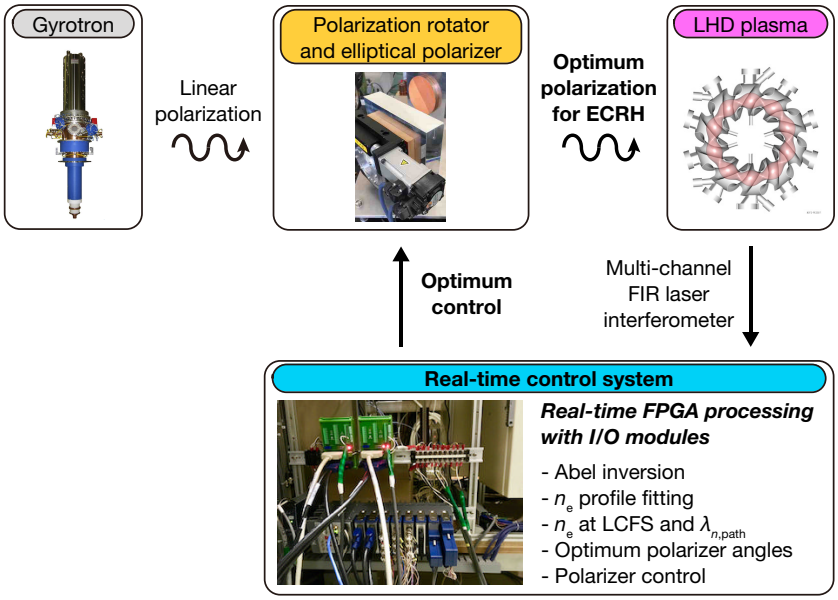

Figure 2: Schematic real-time control system of the incident EC wave polarization.

speed is 6000 rpm. Then the motor is connected to motion control modules NI 9512 and NI 9930P installed on cRIO and rotation of the two polarizers is smoothly and automatically controlled in real time without a control error through the LabVIEW SoftMotion Module.

Voltage signals equivalent to line-integrated electron density measured with the FIR laser interferometer are inputted into cRIO through a newly-made direct-current offset cancellation circuit. Since six channels are receivable by the circuit at present, the six channels of the FIR laser interferometer measured at major radii of R = 3.759, 3.849, 3.939, 4.029, 4.119, and 4.209 m are used to cover sufficiently the peripheral region of LHD plasmas. The core region of LHD plasmas are not fully covered but the selected area of the measurement is sufficient for experiments to realize optimum incident EC wave polarization because the ratio between the O mode and the X mode is determined during propagation on the peripheral region under the density range shown in Fig. 1. Abel inversion to the measured line-integrated electron density is implemented in FPGA as a simple matrix operation that is determined using the geometrical relationship between the observed radii and a plasma equilibrium [12], where the magnetic flux surfaces are approximated elliptic for simplicity because there is no method at present to calculate equilibria of LHD plasmas in real time. More accurate matrix operation is expected if the 3D equilibrium mapping [13] is possible in real time. The discrete electron density profile after the Abel inversion is fitted to a polynomial function with eighth even degree as is done for the electron density profile measured with the Thomson scattering diagnostics. The fitting is implemented in FPGA as the pseudo-inverse matrix operation to provide a least squares solution. The matrix is also determined only using the relationship between the observed radii and the plasma equilibrium. Then, the two parameters $(n_{\mathrm{e,LCFS}}, \lambda_{n,\mathrm{path}})$ regarding the peripheral density profile outside the LCFS are calculated from the fitted electron density profile, which give the polarizer rotation angles to realize the optimum incident EC wave polarization.

In order to evaluate the polarizer control performance, rotation of the two polarizers was controlled to follow sinusoidal command signals for different frequencies, as shown in Fig. 3. The peak-to-peak amplitude of the command signals was set at 30° since the rotation of 30° at most can cover all the optimum polarization states. The execution time of one control loop was maintained approximately 7 ms during the control. The maximum deviation angle per loop was restricted to 9° in terms of the polarizer motion performance. It is confirmed that the two polarizers can follow 0.1 Hz sinusoidal command signals, while higher sinusoidal frequencies give rise to increased control delay as well as decreased amplitude. These results indicate that this control system cannot respond to a sudden change in electron density, e.g., by pellet fueling, but it can cover gradual change of electron density observed in most discharges sustained by gas puffing at the LHD.

Then, one typical result of real-time polarization control tests is shown in Fig. 4. Note that the test was not conducted during the LHD experiment. To simulate an LHD plasma discharge, signals of the FIR laser interferometer of the past discharge #130386 were reproduced from the LHD database server. Those signals were outputted from analog output modules in cRIO and then inputted to the developed real-time control system, i.e., to analog input modules in cRIO. The two parameters $(n_{\mathrm{e,LCFS}}, \lambda_{n,\mathrm{path}})$ calculated in real time during the test were shown in Fig. 4(a) and (b), respectively. For comparison, those parameters calculated from the peripheral electron density profiles measured with the Thomson scattering diagnostics are also shown, respectively. Except for comparatively large variation in $\lambda_{n,\mathrm{path}}$ of the processed Thomson scattering diagnostic data, these results show that there is almost no difference between the two

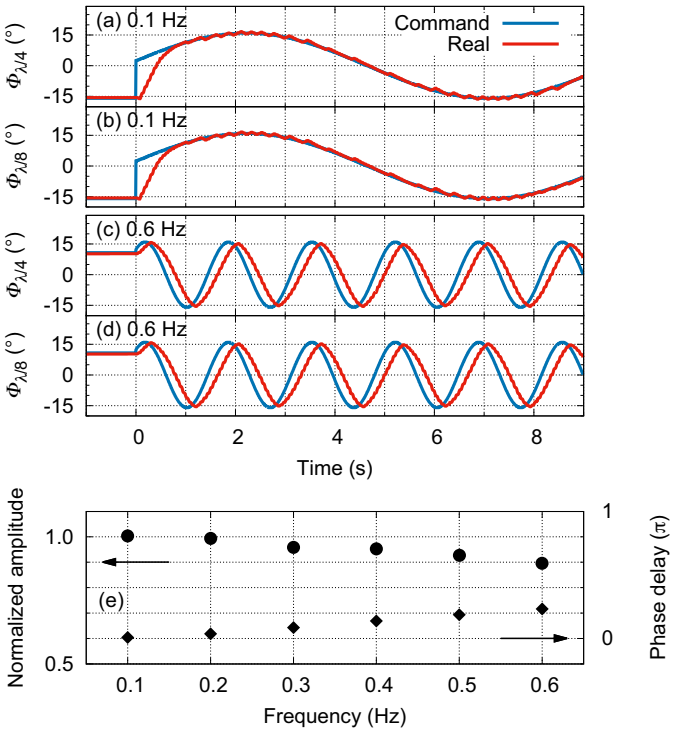

Figure 3: Control test of fast rotation of the two polarizers: Sinusoidal signals are given as commands to the rotation angles of the polarization rotator $\Phi_{\lambda/4}$ and the elliptical polarizer $\Phi_{\lambda/8}$ at the frequencies of (a)(b) 0.1 Hz and (c)(d) 0.6 Hz, respectively, under their peak-to-peak amplitude of 30°. "Real" in the legend denotes the rotation angles of each polarizer. The execution time of one control loop was maintained approximately 7 ms during the control. (e) The rotation angle of the elliptical polarizer normalized by the amplitude of the command signal (the left ordinate) and the phase delay (the right ordinate) as a function of sinusoidal frequency.

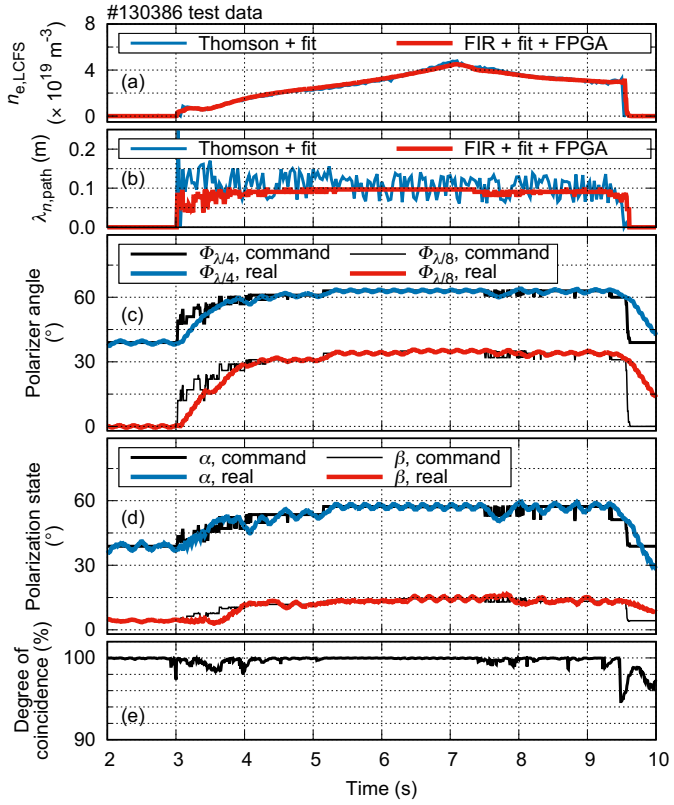

Figure 4: Time evolution of (a) $n_{\mathrm{e,LCFS}}$, (b) $\lambda_{n,\mathrm{path}}$, (c) command rotation angles of the polarization rotator $\Phi_{\lambda/4}$ and the elliptical polarizer $\Phi_{\lambda/8}$ and real rotation angles of those polarizers, (d) command polarization state (α,β) and real polarization state, and (e) the degree of coincidence between the two polarization states, respectively, in a real-time polarization control test. Note that the FIR laser interferometer signals of the shot number #130386 were reproduced from the LHD database server and outputted from analog output modules in cRIO for this test. The two parameters $(n_{\mathrm{e,LCFS}}, \lambda_{n,\mathrm{path}})$ regarding the peripheral electron density profiles measured with the Thomson scattering diagnostics were plotted on (a) and (b), respectively, for comparison.

parameters processed from the FIR laser interferometer signals and those processed from the Thomson scattering diagnostics. This indicates that this real-time control system can provide the appropriate commands for the optimum incident EC wave polarization. Figure 4(c) shows command rotation angles of the polarization rotator and the elliptical polarizer calculated in real time according to the dependence of the optimum polarization on the peripheral density profile, along with real rotation angles of the two polarizers controlled in real time. Figure 4(d) shows the command polarization state and the real polarization state calculated after the test discharge from the command polarizer rotation angles and the real polarizer rotation angles, respectively. Then, the degree of coincidence between the command polarization state and the real polarization state is shown in Fig. 4(e), where the degree of coincidence η is expressed as $\eta = \cos^2(\alpha_{\mathrm{command}} - \alpha_{\mathrm{real}})\cos^2(\beta_{\mathrm{command}} - \beta_{\mathrm{real}}) + \sin^2(\alpha_{\mathrm{command}} - \alpha_{\mathrm{real}})\sin^2(\beta_{\mathrm{command}} + \beta_{\mathrm{real}})$ by using orthogonality of polarization [11]. These results indicate that the polarizers are successfully controlled to follow the commands, so that the optimum polarization states are accordingly realized. It is noted that this real-time control system can function properly not only in short-pulse discharges such as this test discharge of the duration time of almost 10 s but also in long-pulse discharges for steady state operations as long as the FIR laser interferometer signals are obtained. In addition, the electron density signals with the FIR laser interferometer are considered to be replaceable with some estimated density profiles as inputs to the control system when installing diagnostics is restricted in future fusion reactors.

3. Real-time polarization control experiments on the LHD

In order to obtain and sustain maximum absorbed power in ECRH, real-time control of the incident polarization of the 77 GHz EC wave from the 5.5-U port was demonstrated in LHD plasma discharges sustained by other ECRH. Figure 5 shows a typical result of the polarization optimization control. The polarizer rotation angles for the optimum polarization states were decided in real time from the beginning of the discharge according to fast calculation of the peripheral density profile. The polarizer motion control was conducted from $t = 5$ s in comparison to no motion control with the fixed polarization from the beginning of the discharge.

Figure 6 shows time evolution of absorbed power of the 5.5-U EC wave for relatively low-density plasma of

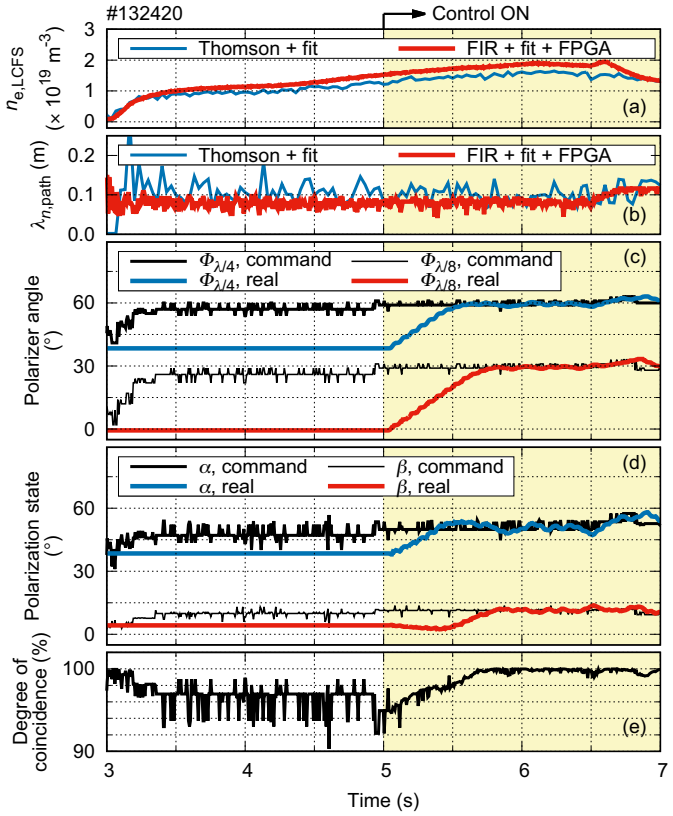

Figure 5: Typical result of polarization optimization control: Lines are plotted as in Fig. 4. The polarizer motion control was conducted from t = 5 s.

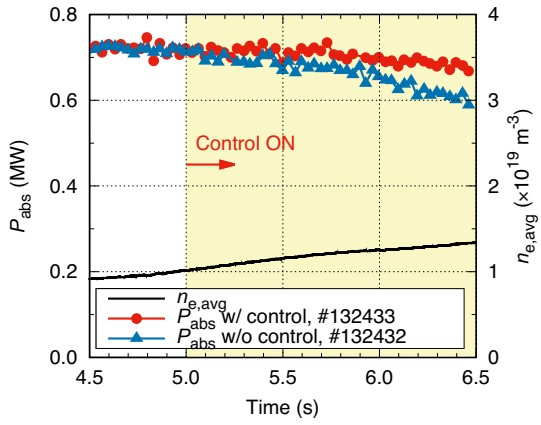

Figure 6: Time evolution of absorbed power of the 5.5-U 77 GHz EC wave for relatively low-density plasma of line-averaged electron density of $\sim 1 \times 10^{19}$ m^{-3} in the cases with and without the polarizer motion control from t = 5 s.

line-averaged electron density of $\sim 1 \times 10^{19}$ m^{-3} in the cases with and without the polarizer motion control. The fundamental O-mode cutoff density is 7.4×10^{19} m^{-3} for 77 GHz, so that refraction of the EC wave can be suppressed. The 5.5-U 77 GHz ECRH power is modulated at the frequency of 15 Hz in order to evaluate the absorbed power from change of the plasma stored energy at on/off timings [14]. The result shows that the absorbed power was maintained high successfully due to the polarization optimization control, while the absorbed power in the case without the control decreased due to slight increase in electron density.

On the other hand, Fig. 7 shows time evolution of the absorbed power during density ramp-up to $\sim 3 \times 10^{19}$ m^{-3}. A difference in absorbed power between the cases with and without the control was observed, although the difference was comparatively smaller than that in the case of the relatively low-density plasma. The mode content analysis with LHDGauss was carried out using the post-processing 3D equilibrium mapping with the Thomson scattering diagnostics, as shown in Fig. 8. The result shows that the O mode purity is increased from almost 90% to 100% due to the control from t = 5 s, indicating that the pure O mode is excited and maintained during the control. Since the X-mode EC wave is reflected at the R cutoff layer in front of the EC resonance layer in this experiment condition, excitation of the pure O mode contributes to maximum first-pass absorption of the EC wave. However, the decreased experimentally evaluated absorbed power along with the small difference in the absorbed power between the cases with and without the control, accompanied by a gradual increase in electron density, suggests

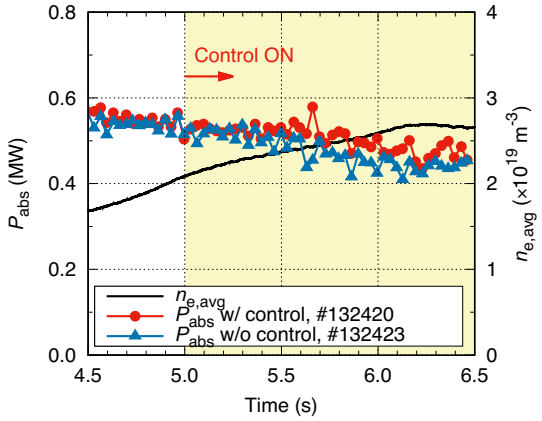

Figure 7: Time evolution of absorbed power of the 5.5-U 77 GHz EC wave during density ramp-up to $\sim 3 \times 10^{19}$ m^{-3} in the cases with and without the polarizer motion control from t = 5 s.

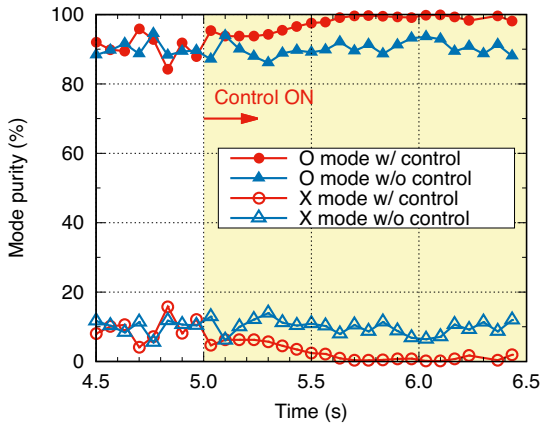

Figure 8: Time evolution of O/X-mode purity analyzed on the same discharges as in Fig. 7.

that high density plasmas give rise to refraction of the first-pass O-mode EC wave, thereby decreasing the first-pass absorption component. Thus, the effect of multi-pass absorption cannot be neglected, although it is difficult to optimize polarization of the second-pass EC wave under the present situation. An effective way to reduce the stray radiation due to multi-pass reflection is either a combination or an integration of EC wave polarization control and deposition location control within the first pass, which is a future work.

4. Conclusions

In order to excite the pure O mode or the pure X mode at the EC resonance layer, a plasma peripheral region with finite density gradients and strong magnetic shear outside the LCFS is taken into account on the LHD. The ray-tracing code LHDGauss, which includes calculation of the O/X-mode ratio by solving the 1D full-wave equation along propagation, helps to search the optimum incident EC wave polarization to excite the pure O/X mode. The real-time control system of the incident EC wave polarization was successfully developed with FPGA that processes in real time the peripheral density profile and optimum control of the polarizers on the transmission line for the 77 GHz wave launched from the 5.5-U port. The real-time polarization control experiment on the LHD demonstrates that absorbed power of the EC wave is successfully maintained higher in a relatively low-density plasma because the pure O mode is excited due to the optimized polarization for the first-pass absorption. Not only the polarization control but also deposition location control can be helpful in achieving full absorption of the EC wave within the first pass even for high density plasmas.

Acknowledgments

The authors gratefully acknowledge the LHD Experiment Group for their operation of the LHD. This work was supported in part by the National Institute for Fusion Science under the grant ULRR027 and by JSPS KAKENHI Grant Number 16K18338.

References

[1] Y. Takeiri *et al*., Extension of the operational regime of the LHD towards a deuterium experiment, Nucl. Fusion 57 (2017) 102023.
[2] H. Takahashi *et al*., Extension of operational regime in high-temperature plasmas and effect of ECRH on ion thermal transport in the LHD, Nucl. Fusion 57 (2017) 086029.
[3] T. Ii Tsujimura *et al*., Development and application of a ray-tracing code integrating with 3D equilibrium mapping in the LHD ECH experiments, Nucl. Fusion 55 (2015) 123019.
[4] T. I. Tsujimura *et al*., Impact of the LHD peripheral region and the magnetic axis shift on optimal on-axis ECRH injection for high-electron-temperature plasmas, Preprint: 2016 IAEA Fusion Energy Conf. (Kyoto, Japan) IAEA-CN-234-0083 (`https://nucleus.iaea.org/sites/fusionportal/Shared%20Documents/FEC%202016/fec2016-preprints/preprint0083.pdf`).
[5] T. I. Tsujimura *et al*., Optimization of incident EC wave polarization in real-time polarization scan experiments on LHD, Plasma Fusion Res. 11 (2016) 2402016.
[6] D. Wagner *et al*., Feed forward polarization control during ECRH discharges at ASDEX Upgrade, Fusion Sci. Technol. 58 (2010) 658-665.
[7] M. Reich *et al*., Real-time beam tracing for control of the deposition location of electron cyclotron waves, Fusion Eng. Des. 100 (2015) 73-80.
[8] K. Okada *et al*., Development of fast steering mirror control system for plasma heating and diagnostics, Rev. Sci. Instrum. 85 (2014) 11E811.
[9] F. Felici *et al*., Feedback control of ECRH polarization on LHD, Nucl. Fusion 50 (2010) 105003.
[10] T. Akiyama *et al*., Interferometer systems on LHD, Fusion Sci. Technol. 58 (2010) 352-363.
[11] T. Ii *et al*., Design of polarizers for a mega-watt long-pulse millimeter-wave transmission line on the large helical device, Rev. Sci. Instrum. 86 (2015) 023502.
[12] Y. T. Cho, S.-J. Na, Applications of Abel inversion in real-time calculations for circularly and elliptically symmetric radiation sources, Meas. Sci. Technol. 16 (2005) 878-884.
[13] C. Suzuki *et al*., Development and application of real-time magnetic coordinate mapping system in the Large Helical Device, Plasma Phys. Control. Fusion 55 (2013) 014016.
[14] R. Makino *et al*., ECH absorbed power evaluation method compensated for temporal response of diamagnetic flux measurements on LHD, JPS Conf. Proc. 1 (2014) 015034, Proc. 12th Asia Pacific Physics Conf.